Supporting information for

Time-resolved photoluminescence in gold nanoantennas

Emilie Sakat[1,+], Ilaria Bargigia[2], Michele Celebrano[1], Andrea Cattoni[3], Stéphane Collin[3], Daniele Brida[4], Marco Finazzi[1], Cosimo D'Andrea[1,2], Paolo Biagioni[1,]*

[1] *Dipartimento di Fisica, Politecnico di Milano, piazza Leonardo da Vinci 32, 20133 Milano, Italy.*

[2] *Center for Nano-Science and Technology @Polimi, Istituto Italiano di Tecnologia, via G. Pascoli 70/3, 20133 Milano, Italy.*

[3] *Laboratoire de Photonique et de Nanostructures, CNRS, Université Paris-Saclay, route de Nozay, F-91460 Marcoussis, France.*

[4] *Department of Physics and Center for Applied Photonics, University of Konstanz, D-78457 Konstanz, Germany.*

[*] to whom correspondence should be addressed: paolo.biagioni@polimi.it

[+] current address: Institut d'Optique Graduate School, Bâtiment 503 - Centre Scientifique d'Orsay 91403 Orsay Cedex

Estimation of the electron temperature after pulse excitation

In order to evaluate the temperature of the hot thermalized electron bath right after pulsed excitation, we applied a standard two-temperature model [R1-R3]:

$$C_{\mathrm{e}}(T_{\mathrm{e}})\frac{dT_{\mathrm{e}}}{dt} = -g(T_{\mathrm{e}} - T_{\mathrm{l}}) + \frac{E_0}{\sqrt{\pi}\sigma_{\mathrm{L}}} e^{-\frac{t^2}{\sigma_{\mathrm{L}}^2}},$$

$$C_{\mathrm{l}}\frac{dT_{\mathrm{l}}}{dt} = g(T_{\mathrm{e}} - T_{\mathrm{l}}) - \frac{T_{\mathrm{l}} - T_{\mathrm{amb}}}{\tau_{\mathrm{S}}},$$

where T_{e} and T_{l} are the electron and lattice temperature, respectively, $C_{\mathrm{e}}(T_{\mathrm{e}}) = \xi T_{\mathrm{e}}$ ($\xi = 68\ \mathrm{J\,K^{-2}\,m^{-3}}$) is the temperature-dependent electron heat capacity per unit volume, $C_{\mathrm{l}} = 2.5 \times 10^6\ \mathrm{J\,K^{-1}\,m^{-3}}$ is the lattice heat capacity per unit volume, $g = 2.2\ \mathrm{W\,K^{-1}\,m^{-3}}$ is the electron-phonon coupling constant, E_0 is the density of energy absorbed by the sample, σ_L is the temporal pulse-width and τ_S is the time-scale for energy transfer to the ambient ($T_{\mathrm{amb}} = 298$ K). Our pulse width is $\sigma_{\mathrm{L}} \cong 0.15$ ps and for simplicity we assume $\tau_{\mathrm{S}} \approx 400$ ps. We note, however, that τ_{S} does not influence the dynamics on the ps time-scale right after excitation, thus we do not need to precisely estimate this parameter. We then evaluate the absorption by the resonant antennas with the finite-difference time-domain method [R4] and we exploit the two-temperature model to calculate the electron and lattice temperatures for the three different power levels employed in Figure 4a of the main text, also taking the throughput of the objective into account. The results in Figure S1 demonstrate that, upon pulsed excitation, the electron bath thermalizes to a temperature that depends on the impinging power and can be as high as about 2500 K above T_{amb}. It should be noted, however, that this estimation, which would require a precise knowledge of the impinging fluence and of the absorption cross sections of the nanoantennas, suffers from a significant uncertainty.

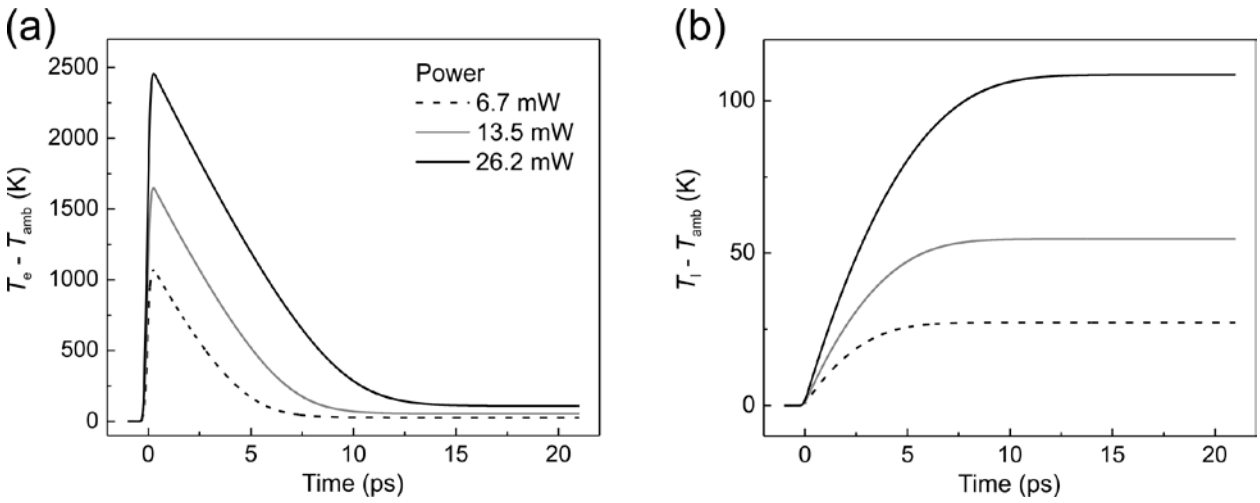

Figure S1 (a) Variation in the electron temperature as a function of time calculated with the two-temperature model for the three different average excitation powers employed in Figure 4a in the main text; (b) variation in the lattice temperature as a function of time from the same simulations.

Another notable feature of the simulation results is the possibility to evaluate not only the maximum temperature but also the relaxation time of the thermalized electron population. In Figure S2 we plot the relaxation time τ (defined as the time required for $T_e - T_{amb}$ to decrease by 50%) as a function of the excitation power. It is seen that higher initial temperatures lead to longer relaxation dynamics with values on the ps time-scale that, given the overall uncertainty, are in fair qualitative agreement with the ps dynamics experimentally observed in Figure 4a of the main text for the resonant antennas.

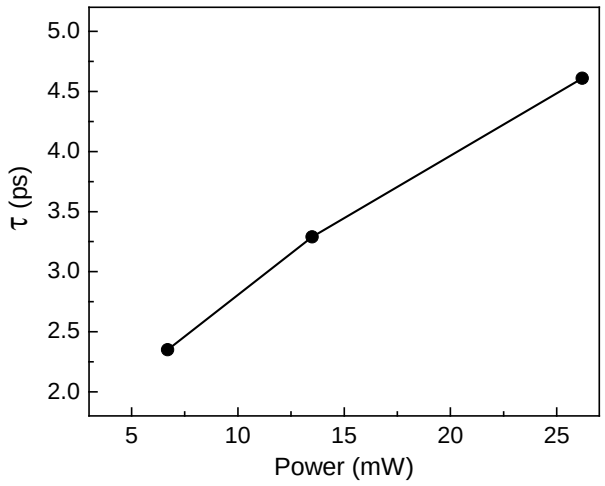

Figure S2 Relaxation time τ of the thermalized electron population calculated from the two-temperature model for the three levels of average power employed for the experiment of Figure 4a in the main text.

Supplementary references:

[R1] Elsayed-Ali, H. E.; Norris, T. B.; Pessot, M. A.; Mourou, G. A. Time-resolved observation of electron-phonon relaxation in copper. *Phys. Rev. Lett.* **1987**, 58, 1212.

[R2] Schoenlein, R. W.; Lin, W. Z.; Fujimoto, J. G.; Eesley, G. L. Femtosecond studies of nonequilibrium electronic processes in metals. *Phys. Rev. Lett.* **1987**, 58, 1680.

[R3] Sun, C.-K., Vallée, F.; Acioli, L.; Ippen, E. P.; Fujimoto, J. G. Femtosecond investigation of electron thermalization in gold. *Phys. Rev. B* **1993**, 48, 12365(R).

[R4] FDTD Solutions, Lumerical Inc., Canada